The Journal of Experimental Biology 211, 1148-1162
Published by The Company of Biologists 2008
doi:10.1242/jeb.012419

Variability in forelimb bone strains during non-steady locomotor activities in goats

Carlos A. Moreno[1,*], Russell P. Main[2] and Andrew A. Biewener[1]

[1]Concord Field Station, Department of Organismic and Evolutionary Biology, Harvard University, 100 Old Causeway Road, Bedford, MA 01730, USA and [2]Sibley School of Mechanical and Aerospace Engineering, 222 Upson Hall, Cornell University, Ithaca, NY 14853, USA

*Author for correspondence (e-mail: cmoreno@oeb.harvard.edu)

Accepted 4 February 2008

SUMMARY

The purpose of this study was to investigate the effects of non-steady locomotor activities on load predictability in two goat forelimb bones and to explore the degree to which bone curvature influences load predictability. We measured *in vivo* bone strains in the radius and metacarpus of juvenile goats performing a variety of natural behaviors in an outdoor arena and compared these strain magnitudes and loading patterns with those measured during steady-state treadmill locomotion. We sought to test two hypotheses: our first hypothesis expects an increase in the variability of strain magnitude and pattern during outdoor non-steady behavior when compared to treadmill locomotion. Our second hypothesis was that the curved radius experiences higher peak strains but less variability during non-steady activities than the straighter metacarpus. We found that unsteady, outdoor locomotion generally caused more variable strain patterns (consistent with the first hypothesis), but not more variable strain magnitudes, than treadmill locomotion in both bones. During outdoor locomotion, higher magnitude strain events in the radius showed more constrained loading patterns than in the metacarpus (consistent with the second hypothesis). In addition to the radius experiencing significantly greater bending strains compared to the straighter metacarpus, these results support the idea of a trade-off between increased predictability of loading pattern and increased bending-induced strain. Strain magnitudes recorded during both outdoor and treadmill locomotion showed a lognormal frequency distribution, but the outdoor bone strain distributions had a greater range because they included high magnitude loading events that did not occur during steady treadmill locomotion.

Key words: bone strain, variability, curvature, non-steady locomotion, skeletal mechanics, goat.

INTRODUCTION

Limb bones in tetrapods provide the structural framework by which forces are transmitted for body support and movement. These forces include the loads associated with steady locomotion, which have been the focus of most past studies, as well as those that occur during non-steady locomotor events. Non-steady events are likely to be particularly important for animals operating in their natural habitat. Consequently, it is important to understand how bone loading may change as a function of non-steady *versus* steady locomotor activity. The goal of our study, therefore, was to address this question by recording *in vivo* strains in two principal forelimb bones of African pygmy goats (*Capra hircus*) across a range of locomotor activity.

In contrast to non-steady locomotion, limb bone strains have been measured in a variety of animals during steady, level locomotion across a range of gaits and speeds (Lanyon, 1976; Carter et al., 1980; Biewener and Taylor, 1986; Blob and Biewener, 1999; Lieberman et al., 2003). These studies show that strain magnitudes, measured at a bone's midshaft, increase with speed, consistent with increased limb loading (Biewener et al., 1983a; Main and Biewener, 2004). However, the pattern and distribution of strain, quantified in terms of the orientation of principal strains and the distribution of axial, bending and/or shear strain components measured at the time of peak strain, tend to remain fairly uniform across different speeds and gaits (Rubin and Lanyon, 1982; Biewener and Taylor, 1986; Main and Biewener, 2004). It is important to note that cross-sectional strain patterns often change over the course of a loading cycle, with substantial shifts in the location and orientation of the neutral axis (Gross et al., 1992; Biewener and Dial, 1995; Main and Biewener, 2004). Nevertheless, it is generally believed that bone shape and mechanical function are most strongly influenced by the peak strains experienced by a bone over some history of loading cycles (Carter, 1987; Mosley et al., 1997; Robling et al., 2001; Burr et al., 2002). Previous work, therefore, has provided insight into the underlying structural design of limb bones in relation to steady, forward locomotion but has largely ignored the pattern of bone strains experienced during non-steady activity.

Animals must be capable of executing vigorous non-steady behaviors, such as rapid turning and sudden accelerations, which are likely to be especially critical during predator–prey interactions. Consequently, adequate support of mechanical loads during these more variable, though perhaps less frequent, activities is likely to be as important to skeletal design as support of loads during steady locomotion. Indeed, peak stresses determined from *in vivo* bone strains in the horse radius, metacarpus and tibia (Biewener et al., 1983a; Biewener et al., 1988) during jumping were significantly greater, and the distribution of strains more variable, than with steady-speed locomotion.

Variation in bone strain patterns reflects the predictability of limb and bone loading regimes. Load predictability, in turn, is probably an important determinant of a structure's safety factor, often defined as the ratio of the structure's breaking or yield strength relative to the expected maximum load during use. Other factors, such as the cost of building and maintaining the structure, and the cost of failure are also important determinants of a structure's safety factor

(Alexander, 1981). With increased variation in loading (reduced predictability) the safety factor of a structure, such as a limb bone, can be expected to decrease. Consequently, evaluating peak bone strains and strain distributions across a range of locomotor activities is important for assessing skeletal safety factors.

Bone shape probably influences strain patterns by predisposing different surfaces of the bone to certain types of strain. For example, many long bones are curved along their length, and although this may increase the peak strains developed within the bone due to increased bending loads, it may also improve a bone's loading predictability (Lanyon, 1987; Bertram and Biewener, 1988; Bertram and Biewener, 1992) by limiting the principal direction of bending to a particular plane. In a comparison of midshaft bone strains in the horse radius (curved) and the metacarpus (straight), strain patterns during steady locomotion and jumping were found to be more variable in the straighter metacarpus (Biewener et al., 1983a). In addition, the uniform anatomical arrangement of muscles, tendons and ligaments, which transmit substantial forces to the skeleton, might also be expected to limit the range of loads that a bone experiences, favoring increased load predictability.

To assess how bone morphology might influence, and possibly constrain, functional loading patterns, we compared *in vivo* bone strains acting in the midshaft of the radius and metacarpus of juvenile goats performing a variety of natural behaviors in an outdoor arena and compared them with strains measured during steady treadmill locomotion. We hypothesized that strains measured during outdoor non-steady behaviors would be more variable in pattern and magnitude than those measured during treadmill locomotion. Similar to horses and other ungulates (Bertram and Biewener, 1992), goats have a curved, caudally concave radius and a fairly straight metacarpus. Consequently, we also hypothesized that during non-steady activities the curved radius would experience less variability in strain pattern and higher peak strains than the straighter metacarpus.

MATERIALS AND METHODS

Animals and training

The seven juvenile African pygmy goats (*Capra hircus*, L.), ages 4–42 weeks (age 16.9±16.1 weeks; mass 8.21±2.7 kg; mean ± s.d.), included in the experiment were bred and reared in open paddocks at the Concord Field Station (Harvard University). Goats of this age are generally more active and more easily persuaded to move about than older animals. Although the variation in mass is low, we were concerned about the variation in age, so we tested for effects of age on cranio-caudal and medio-lateral curvature, cross-sectional eccentricity, and curvature-to-length ratios. There were no significant differences across age for these geometric parameters, so we were confident including all juvenile goats in our experiment. The animals were trained to run on a motorized treadmill (belt dimensions: 0.4 m×2.5 m; width×length) for approximately 1 week prior to the collection of strain data, and were considered trained when they could maintain a steady gait while walking, trotting and galloping at different speeds for periods of up to 5 min. Animal care, training and experimental procedures were approved by the Institutional Animal Care and Use Committee at Harvard University.

Recording of ground reaction forces

Pre-operative ground reaction forces (GRFs) were collected while the animals walked, trotted and galloped steadily across a level runway with two embedded force platforms (0.4 m×0.6 m; model 9286A; Kistler, Amherst, NY, USA) set flush with the runway's surface. The next day, surgery was performed to attach the strain gauges. The following day, after collecting strain data from both outdoor and treadmill trials, post-operative ground reaction forces were recorded using the same runway. The pre-operative and post-operative GRFs were zeroed and filtered and the mean peak vertical GRF was found for each of the three gaits, using a custom MATLAB program (The Mathworks, Inc., Natick, MA, USA). The ratio of pre-operative to post-operative peak GRF was used as a correction factor by which the measured strains were multiplied to account for lameness due to surgery.

Surgery

Each goat was surgically instrumented with strain gauges on either the radius, metacarpus, or in the case of two animals, the left radius and the right metacarpus. The animals were sedated with a mixture of ketamine (4 mg kg^{-1}) and xylazine (1 mg kg^{-1}) administered intravenously (jugular), then intubated and maintained under general anesthesia at 0.5–2.0% isoflurane. For the implantation of strain gauges on the radius, a 4–5 cm incision was made over the medial aspect of the forearm. The lead wires from the gauges were then fed subcutaneously from an opening near the shoulder to the medial opening on the limb. Skin and underlying fascia were retracted to expose the bone's midshaft. The periosteum at the midshaft was removed using a scalpel and a periosteal elevator and the bone surface lightly scraped, cleaned and dried using methyl-ethyl-ketone. Rosette strain gauges (FRA-1-11; Tokyo Sokki Kenkyujo Co., Ltd, Tokyo, Japan) were attached to the cranial and caudal midshaft surfaces and a single-element gauge (FLA-1-11) to the medial surface of the bone using self-catalyzing cyanoacrylate adhesive. Strain gauge preparation was similar to previous studies (Lanyon, 1976; Biewener, 1992). A similar approach and procedure were used to attach rosette strain gauges to the cranial and caudal surfaces and a single-element gauge to the medial surface of the metacarpus. In this case, gauge wires were fed subcutaneously from an opening near the shoulder to a lateral opening on the limb, passing outside the skin over the wrist to a medial incision over the metacarpus. Gauges were bonded to the midshaft of each bone because this is the location at which the greatest strains occur in long bones subjected to significant bending (Biewener and Taylor, 1986). Following gauge attachment, the skin openings were sutured with 3-0 vicryl and the connector secured to the skin overlying the withers with 2-0 vicryl suture. The animals were allowed to recover overnight before experimental recordings were made, and flunixin (1 mg kg^{-1}) was administered (intramuscular) every 12 h following surgery to reduce pain.

Outdoor experiment

The outdoor arena consisted of a semi-rectangular area (~20 m^2) enclosed by twisted wire fencing, approximately 1.5 m in height, located beside an observation room where the cameras and equipment were located (Fig. 1). A clear plastic barrier was used to prevent the goats from entering the observation area. A wooden ramp 0.78 m×1.25 m (width×length) with a 21° angle to the ground was placed next to a 0.47 m×0.41 m×0.78 m wooden box such that the goats could run up the ramp and jump off the box, or jump onto the box and run down the ramp. Each trial lasted approximately 30 s and consisted of the experimenter energetically chasing the animal around the outdoor arena with the goal of evoking as wide a range of natural behaviors as possible. The behaviors included straight runs across the arena, turns and dodges, jumps and runs up and down the ramp, as well as braking and accelerating. The goats were at ease running up and down the ramp, and had no difficulty

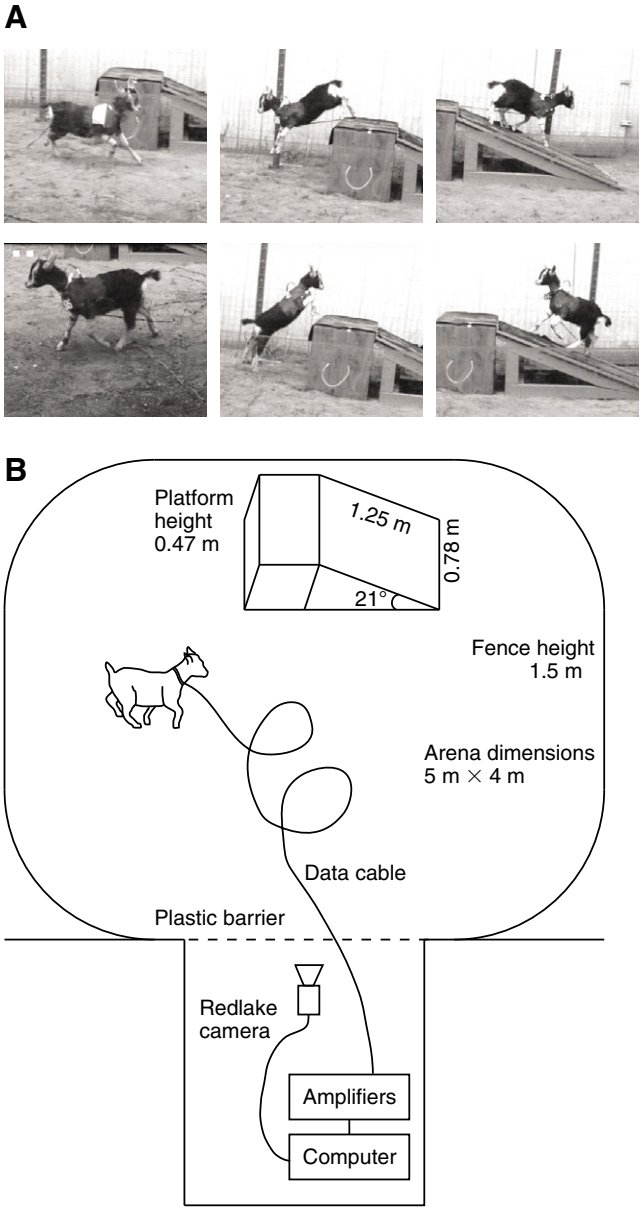

Fig. 1. Outdoor experimental setup. (A) Video stills of outdoor locomotor behaviors, depicting gallops and trots on the level, jumping on to and off of the platform, and running up and down the ramp. (B) Diagram of the outdoor arena showing the location of the ramp and platform. Goats were freely chased around in the arena while trailing a data cable to record *in vivo* bone strains. Kinematics were recorded from behind a clear plastic barrier.

jumping onto and off the platform, with minimal signs of limping due to surgery.

Signals from the strain gauges were transmitted *via* lightweight shielded cable (60 g m^{-1}) to a bridge amplifier (Vishay 2120; Micromeasurements, Raleigh, NC, USA). Voltage outputs from the bridge amplifiers were recorded to a computer using a 12-bit A/D converter and Axoscope software (version 8.0; Axon Instruments, Inc., Union City, CA, USA). Prior to experimental recordings, each channel of the bridge amplifier was balanced and calibrated (1000 $\mu\epsilon$ shunt calibration) while the animal was held suspended in the air with no weight on its limbs. The overall locomotor behaviors of each goat were filmed from the observation room using a high speed digital video camera (Redlake Motionscope PCI; San Diego, CA USA) at 60 Hz, allowing hoof contact times to be recorded and the locomotor behavior associated with each footfall of the experimental limb to be classified.

Behaviors

Each behavior was first classified as a walk, trot, gallop or jump. The walks, trots and gallops that occurred on level ground were further classified as steady gallops, steady walks/trots, accelerations or decelerations. The rest of the walks, trots and gallops were categorized as either uphill or downhill. The jumps were divided into high-force jumping behaviors (landing down/jumping up) and low-force jumping behaviors (landing up/jumping down). This yielded eight possible behavior combinations. Strain data and hoof contact times for footfalls of the experimental limb were recorded while the animal was performing one of these definable behaviors. Footfalls during behaviors that did not fall into one of these categories (discontinuous, non-forward locomotor behaviors such as slipping, backing up, stepping sideways, shifting weight, slowly turning in place, etc) did not result in consistent strain traces that would allow us to find meaningful peak strains, or the strains were of such low magnitude that the signal was considered unreliable, so these footfalls were not analyzed.

Treadmill locomotion

After the outdoor strain data collection trials, the goats were led indoors and made to walk, trot and gallop at a range of speeds (1.1–3.8 m s^{-1}) on a motorized treadmill. High speed digital video (Redlake Motionscope) was taken from a lateral aspect at 125 Hz to record the foot-down and foot-off times of the experimental limb. Bone strains were recorded from the radius, the metacarpus, or both bones simultaneously (depending on the animal and bones that were instrumented with strain gauges), while the goat ran at controlled speeds. After strain data and post-operative GRF data were collected, the animals were euthanized by an injection of sodium pentobarbital (150 mg kg^{-1}; intravenous, jugular). The instrumented bones were dissected from the limbs and the orientations of the strain gauges relative to the long axis of the bone measured using digital photographs of the dissected bone. The curvatures of the bones (Fig. 2B) were measured using a previously described technique (Bertram and Biewener, 1992; Main and Biewener, 2004).

In vivo strain analysis

Each outdoor trial yielded 15–40 footfalls that were analyzed. For each treadmill trial, data from five consecutive foot contacts were chosen in which the goat moved at a steady pace on the treadmill. The number of samples recorded from the six bone sites (cranial, caudal and medial cortices of the metacarpus and radius) for each goat is shown in Table 1. Note that some of the cells are empty because in certain animals data was only recorded from one bone; in other cases, data was recorded at an earlier phase of the study when measurements focused only on the radius. Other missing cells are a result of faulty strain gauge signals which were not analyzed.

The raw strain data were analyzed using a custom MATLAB program (Main and Biewener, 2004). Raw data were first filtered using a fourth order Butterworth filter with a cutoff frequency of 125 Hz. The data were then zeroed by subtracting the average strain during swing phase (when the voltage changes are minimal) from the filtered data, then the voltages were converted to microstrain ($\mu\epsilon$, or strain $\times 10^{-6}$) using the 1000 $\mu\epsilon$ shunt-calibration. For the rosette strain gauges, standard equations that assume a uniaxial

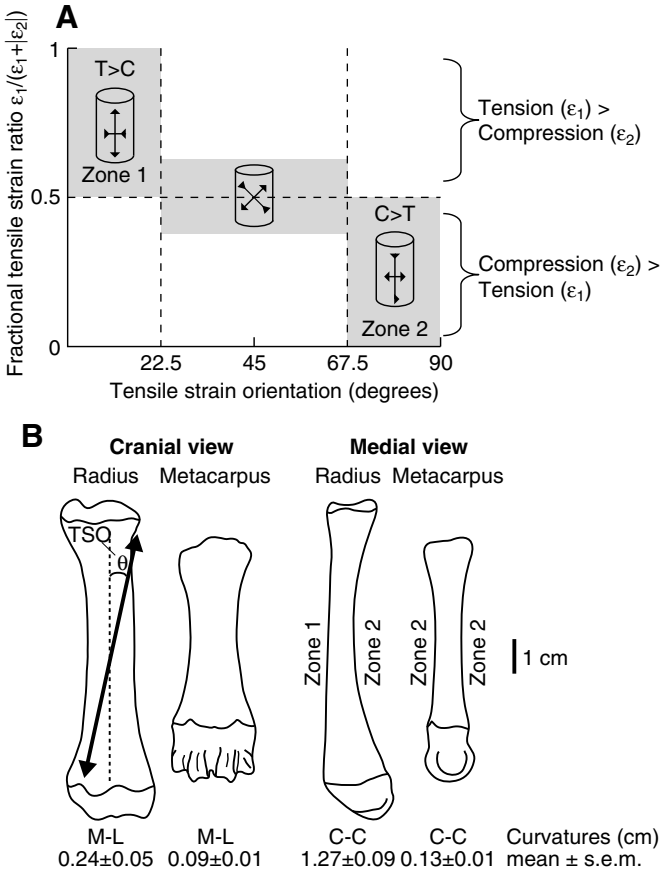

Fig. 2. (A) Parameter space used to evaluate and represent the variability in loading pattern. The x axis is the orientation of the tensile principal strain relative to the long axis of the bone (TSO). The y axis is the fractional measure of the dominant strain type (FTSR): values greater than 0.5 indicate that tension>compression whereas values less than 0.5 indicate compression>tension. The broken outlines delineate zones in which we expect the majority of loading events to occur, either tension>compression and TSO aligned near the long axis (zone 1), or compression>tension and principal compression angle aligned near the long axis (TSO closer to 90°; zone 2). Between 22.5° and 67.5° the TSO is closer to the diagonal (45°) than to either the long or transverse axis of the bone, and compression and tension magnitudes are approximately equal (e.g. this would be the case for torsion). (B) Illustrations of the radius and metacarpus, with medio-lateral (M-L) and cranio-caudal (C-C) curvature values from each aspect. The cranial and caudal surfaces are labeled with the loading zone where strain data from that surface would be expected to occur for a typical loading cycle. Tensile strain orientation (TSO) is the angle (θ) between the principal tensile strain and the longitudinal axis. All illustrations are drawn to scale.

planar state of strain were used to convert the zeroed and calibrated strains into principal tensile and compressive strains. By convention, the principal tensile and compressive strains act perpendicular to one another. From these equations the orientations of the principal tensile strains relative to the long axis of the bone were also found (Fig. 2B). These angles were corrected for any gauge offset found after inspecting the attached gauge on the dissected bone. Principal strains and orientations could only be calculated from rosette strain gauges with three functioning elements; footfalls in which the gauges had one or more non-functioning elements were not used. The principal strains and the strains recorded from the medial single-element gauges were multiplied by the post-operative correction factor to adjust the strains for post-operative lameness (average correction 1.10±0.05 across animals). This post-operative reduction in limb load probably only affected strain magnitudes and not the overall strain patterns (Main and Biewener, 2004).

For each stance phase, the peak positive (tensile) and negative (compressive) principal strains and their orientations, along with their corresponding principal strains, were recorded for each rosette gauge on the cranial and caudal cortices of the metacarpus and radius. Peak longitudinal strains on the medial surfaces of both bones were also recorded. Because peak principal tension did not necessarily occur at the time of peak principal compression (principal tension tended to peak around 70±17% of stance phase, whereas principal compression peaked around 50±20% of stance; mean ± s.d.), we determined which of the two had the greatest average absolute magnitude for any given behavior category and used the larger and its orientation in further analyses.

Once it was determined whether the peak compression or peak tension was greater during a particular footfall, the degree to which the peak principal strain dominated the corresponding perpendicular strain was quantified by calculating the 'fractional tensile strain ratio' (FTSR) for each footfall:

$$\mathrm{FTSR} = \epsilon_1 / (\epsilon_1 + |\epsilon_2|) , \quad (1)$$

where ϵ_1 and ϵ_2 are the principal tension and compression, respectively. FTSR represents the ratio of the principal tension to the sum of the principal tension and the absolute magnitude of the corresponding principal compression. When principal tension exceeds principal compression, the ratio is between 0.5 and 1, and when compression is greater than tension, the ratio is between 0 and 0.5. This ratio identifies the dominant type of strain for a particular footfall, and its relative dominance. When principal tension equals principal compression (as for pure torsion), FTSR=0.5.

At the time of the largest peak principal strain, the tensile strain orientation (TSO) relative to the bone's long axis was also determined. This value falls between 0° and 90°: if the principal tensile strain is aligned near the long axis of the bone, the angle will fall near 0°, whereas, if the principal compressive strain is aligned close to the long axis, TSO will be closer to 90°. When the TSO associated with a given peak strain lies between 22.5° and 67.5°, then the bone is experiencing primarily off-axis loads, such as torsion, since in these cases the principal tension is acting in an orientation that is closer to 45° than to either the longitudinal or transverse axis of the bone. We plotted FTSR against TSO (Fig. 2A) to evaluate the degree of variability in loading patterns for different bone surfaces in relation to both the dominant strain type and the orientation of the strain relative to the long axis of the bone.

Axial and bending strain components were determined by using the following equations (Main and Biewener, 2004):

$$\epsilon_{\mathrm{axial}} = (\epsilon_{\mathrm{cranial}} + \epsilon_{\mathrm{caudal}}) / 2 , \quad (2)$$

$$\epsilon_{\mathrm{bending}} = \pm|(\epsilon_{\mathrm{caudal}} - \epsilon_{\mathrm{cranial}}) / 2| , \quad (3)$$

where $\epsilon_{\mathrm{cranial}}$ and $\epsilon_{\mathrm{caudal}}$ are the peak principal strains on the cranial and caudal surfaces of the bones, respectively.

Measures of variability

We quantified the variability in loading pattern for each bone surface in a number of ways. The two-dimensional spread in data points was first determined using the participation ratio (PR), which is the area occupied by data on the 2D scatterplot (Fig. 2A). PR is calculated by dividing the 2D parameter space into a number of bins and assessing the number of bins that contain data points,

Table 1. Individual masses, sample sizes and number of footfalls per bone surface for each goat

		Metacarpus						Radius					
		Outdoor			Treadmill			Outdoor			Treadmill		
Goat	Mass (kg)	Cr	Ca	Md	Cr	Ca	Md	Cr	Ca	Md	Cr	Ca	Md
1	8.18		62	193		29	4		180		19	29	
2	11.20							240	250	263	30	30	30
3	11.60	133	231	237			40			222			40
4	9.24	245	214		30	30	30						
5	7.40	118	176	229	35	35	35	200	203	236	35	35	35
6	4.94							142	237	244	50	50	50
7	4.90							233	231	245	30	30	30
Total footfalls		486	683	659	65	94	109	815	1101	1210	164	174	185
N		3	4	3	2	3	4	4	5	5	5	5	5

Bone surfaces: Cr, cranial; Ca, caudal; Md, medial.
Missing data are a result of: (1) earlier phases of the study which included only radius strain data, or (2) unreliable strain gauge data.
Mean mass: 8.21±1.02 kg.

normalized by the number of samples in order to remain robust to sample size (Ciampaglio et al., 2001). The value is dimensionless and can range from 1.0, for which all of the data points lie in one bin, up to the number of bins (2500 in this case). Thus, the lower the PR value, the more constrained the data are in the 2D parameter space. PR gives an indication of the amount of scatter in a group of data on the pattern graphs, and although PR values from two groups cannot be compared statistically using a *t*-test, PR can be found for different individuals and averaged. As another measure of two-dimensional spread in data points the 2D distance to the individual mean (DIM) was determined. This was done by dividing the TSO value of each data point by 90° to scale it from 0 to 1 (to match the FTSR value range) and then calculating the 2D distance from each point to the individual mean for each animal. The average distance to the DIM across the individuals sampled was then determined for each bone surface.

To measure how constrained the loading patterns were to a certain range of strain orientations and strain types, we calculated the percentage of footfalls for each bone surface that landed within the expected zone for a given surface (zone 1 for the cranial radius, zone 2 for the caudal radius, and the cranial and caudal metacarpus; Fig. 2). The two bones were then compared using the average percentage across the cranial and caudal surfaces, where a higher percentage meant less variability and a lower percentage more variability. In addition to considering these composite measures of variability in loading pattern, we also considered the two dimensions (TSO and FTSR) separately, using their variance as a measure of variability (Sokal and Rohlf, 1981).

To quantify variation in strain magnitude frequency distributions, we again used the sample variance as a measure of variability (Sokal and Rohlf, 1981) to compare between groups. To compare variability in axial *versus* bending strain components in the metacarpus and radius, we used the coefficient of variation (CV) of each component.

Statistical analysis

To assess differences in loading pattern variability we compared means of the following parameters between the outdoor and steady treadmill trials: PR, DIM, percent of footfalls in the expected bone loading zone (Fig. 2A), variance in TSO, and variance in FTSR. The variance in TSO and FTSR within individuals was also compared between outdoor and treadmill conditions. To assess differences in strain magnitude between conditions, we compared mean absolute principal strain magnitudes for each surface, as well as the mean magnitudes for the axial and bending strain components for both bones. To investigate strain magnitude variability we compared the variances of the absolute principal strain magnitude distributions and mean coefficients of variation for the axial and bending strain magnitudes.

To test for differences in the means described above, we performed unpaired *t*-tests and non-parametric Mann–Whitney *U*-tests when the variances of two groups were not equal. The *P* values were adjusted using the sequential Bonferroni technique to correct for multiple comparisons (Rice, 1989). To test for differences in variance between conditions (for TSO, FTSR and principal strain distributions), we performed *F*-tests in which we compared the ratio of the variances between two groups to the critical *F* value (Rohlf and Sokal, 1981).

To determine if the strain magnitude frequency distributions fit a lognormal distribution, we performed Kolmogorov–Smirnov Lilliefors 'goodness of fit' tests on the strain magnitudes from each bone surface under both outdoor and treadmill conditions. The sample distribution is considered to be not significantly different from a lognormal curve if $P>0.05$. All statistical tests were performed using SPSS (version 14.0 for Windows; Chicago, IL, USA), except for the goodness of fit tests, which were performed in JMP (version 4; SAS Institute Inc., Cary, NC, USA). Significance threshold was set at $P<0.05$ and values presented in the text are means ± standard error (s.e.m.), unless otherwise noted.

RESULTS

Outdoor behaviors

When chased around the outdoor enclosure the goats performed many more gallops (53% of loading cycles) than any other gait (14% walks, 14% trots and 19% jumps). They often accelerated in one direction, and then quickly dodged in a new direction before coming to a standstill. Representative principal tensile and compressive strains for the caudal surface of the radius during one complete trial (Fig. 3A) show that activity often came in bursts; the animal would dash about for a few steps and then pause before bounding away again. An expanded view of these representative principal strain traces (Fig. 3B) reveals that the strain record varied among different outdoor behaviors. The caudal surface of the radius, similar to the other surfaces tested, experienced the highest strains during decelerating and accelerating gallops – the six footfalls with the greatest compressive strain peaks were three accelerations and three decelerations. On the caudal radius surface the peak compressive strains were greater than peak tensile strains, causing the footfalls from this trial to fall into zone 2 on the 2D scatterplot of loading

pattern (TSO plotted against FTSR, Fig. 3C, filled points). Strains from the cranial surface of the radius for this trial (traces not shown) fell into zone 1 (Fig. 3C, open points).

Treadmill behaviors

The strain records from successive treadmill footfalls were uniform, and, similar to the outdoor footfalls, the gallops generally showed the highest peak strains (Fig. 3D). For the caudal surface of the radius and the cranial and caudal surfaces of the metacarpus the peak compressive strains were greater than the peak tensile strains, causing these footfalls to fall into zone 2 in the pattern scatterplot (not shown in Fig. 3C for this example scatterplot), whereas the cranial surface of the radius experienced peak tensile strains that were greater than the peak compressive strains, causing these footfalls to fall in zone 1 (2D scatterplot again not shown for these representative data). The medial surface of both bones experienced compression. In the case of the radius the peak axial strain magnitudes on the medial surface were approximately equal to the peak principal strains of the caudal surface, whereas in the metacarpus the medial surface experienced compressive strains three

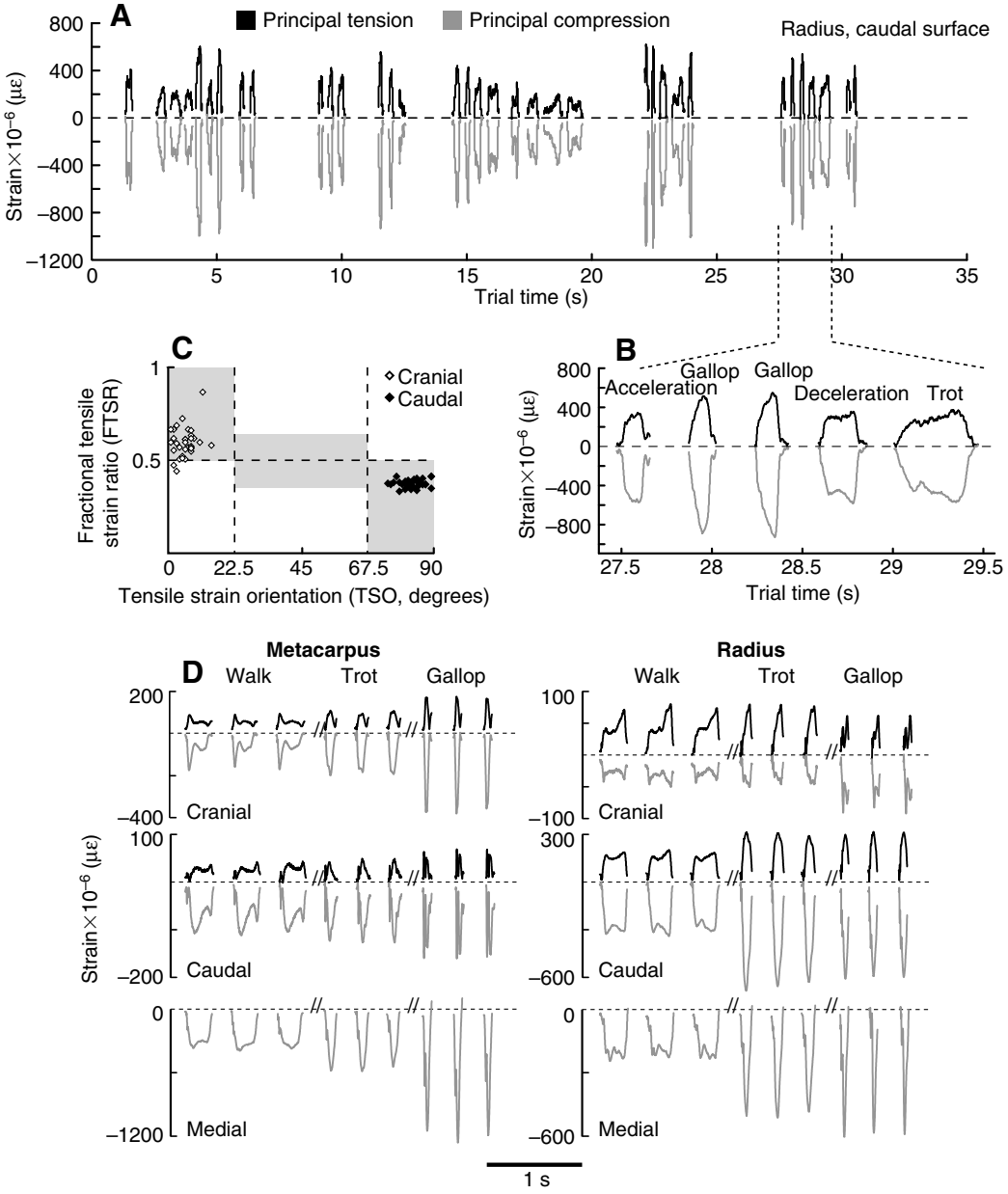

Fig. 3. (A) Representative strain record showing principal tensile (black) and compressive (grey) strains from the caudal surface of the radius during one trial lasting about 30 s. Strains are shown during the contact phase of identified loading cycles (swing phase and non-analyzed footfalls have been discarded). (B) Expanded view of five footfalls, showing a range of natural locomotor behaviors. (C) Two-dimensional scatterplot depicting the loading pattern for this surface (caudal radius, black diamonds), as well as the opposite surface (cranial radius, white diamonds; strain trace not shown), during this representative trial. (D) Principal tensile (black) and compressive (grey) strains for cranial, caudal and medial surfaces (medial surfaces show axial strains) for the metacarpus and radius during representative treadmill footfalls. Each panel shows three consecutive walks, trots and gallops from one goat during different trials. Note the difference in *y* axis scale for each surface.

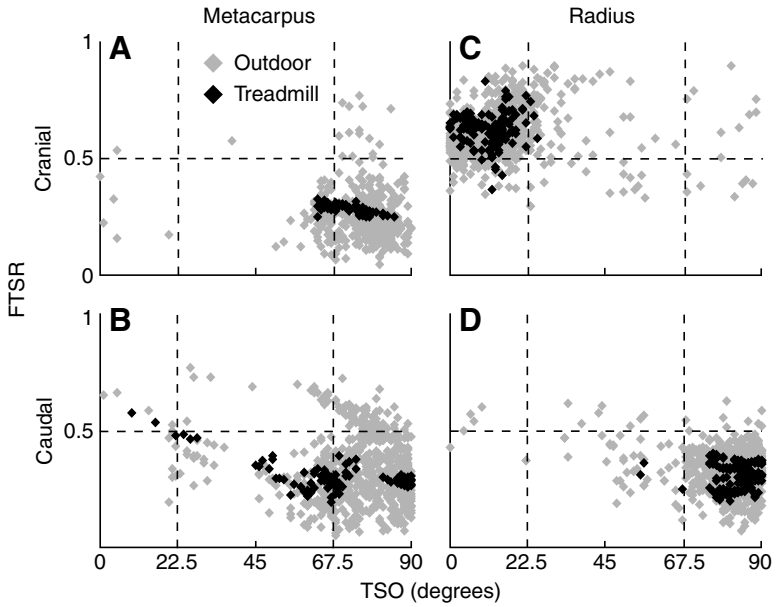

Fig. 4. 2D scatterplot of loading pattern for all loading cycles from outdoor (grey) and treadmill (black) locomotion, showing fractional tensile strain ratio (FTSR) plotted against tensile strain orientation (TSO) for the cranial and caudal midshaft surfaces of both bones. Variability in pattern was greater during outdoor, non-steady behaviors than during steady treadmill locomotion (for descriptive statistics, see Table 2). Mean values for FTSR and TSO were nearly identical between outdoor and treadmill conditions. On average, the radius had a significantly higher percentage of footfalls that landed within the expected loading zones.

to six times greater than the compressive strains of the cranial or caudal surface (Fig. 3D).

Overall strain pattern

To investigate the influence of specific activities on strain loading pattern, we plotted each footfall according to its specific behavior. We found that the behaviors did not cluster in the 2D loading pattern space. All outdoor activities, from walks to gallops to jumps, were spread out evenly (figure not shown), indicating that no particular behavior consistently produced a predictable TSO and FTSR. We also performed a one-way ANOVA to test for an effect of activity on participation ratio. The ANOVA revealed that PR did not differ significantly as a function of activity ($F_{7,60}$=1.41, P=0.22). Thus, in the remainder of our analysis we considered all types of outdoor behaviors together, without regard to the specific behavior shown (i.e. high-force jump *versus* gallop etc.).

The general bone loading patterns for outdoor footfalls were similar to those of treadmill footfalls, with the majority of loading cycles falling in the same zone for both outdoor and treadmill (Fig. 4). For example, the percentage of footfalls in the expected zone during outdoor and treadmill locomotion was 72% and 74% for the cranial surface of the metacarpus, and 53% and 51% for the caudal surface, respectively (Table 2). This was the case for the cranial and caudal surfaces of both forelimb bones (Fig. 4). For outdoor footfalls, the cranial and caudal surfaces of the metacarpus were loaded primarily in compression (FTSR: 0.26±0.01 and 0.33±0.04, respectively) with the principal compression lying closer to the long axis of the bone (TSO: 74±4° and 68±9°, respectively; Table 2). In the radius, the caudal surface was loaded similarly (FTSR: 0.33±0.02; TSO: 81±1°), but the cranial surface was loaded primarily in tension, which acted near the bone's long axis (FTSR: 0.62±0.02; TSO: 14±3°; Table 2).

During treadmill activity (Fig. 4), the metacarpus experienced generally similar loading patterns as observed for the outdoor activities, with the cranial and caudal surfaces experiencing compression (FTSR: 0.28±0.01 and 0.30±0.02, respectively) that

Table 2. Descriptive statistics for measures of loading pattern variability

	Metacarpus				Radius			
	Outdoor		Treadmill		Outdoor		Treadmill	
	Cranial	Caudal	Cranial	Caudal	Cranial	Caudal	Cranial	Caudal
N	3	4	2	3	4	5	5	5
PR	60±10	75±15	10±1	17±5	64±17	51±7	14±4	11±3
Average PR	69±10		14±3		57±8		12±2	
DIM	0.11±0.03	0.14±0.02	0.03±0.001	0.08±0.04	0.11±0.01	0.08±0.01	0.05±0.01	0.05±0.02
Average DIM	0.12±0.02		0.06±0.03		0.09±0.01		0.05±0.01	
% in zone	72±20	53±19	74±26	51±28	81±7	94±2	95±2	98±2
Average %	61.2±13.5		60.1±18.2		88.6±3.7†		96.5±1.6†	
TSO (deg.)	74±4	68±9	72±5	68±11	14±3	81±1	10±3	81±1
FTSR	0.26±0.01	0.33±0.04	0.28±0.01	0.30±0.02	0.62±0.02	0.33±0.02	0.63±0.02	0.31±0.02
Variance TSO (deg.)	12.5±9.4	15.4±6.7	0.98±0.002	11.1±10.3	18.5±3.8	11.6±3.0	1.0±0.36	3.1±1.6
Variance FTSR	11.3±6.6	14.1±2.3	0.23±0.02	4.2±3.1	8.5±3.1	3.7±0.8	2.8±1.5	0.55±0.23

All values are means ± s.e.m.; *N*=number of individuals.

Composite measures of variability: PR, participation ratio: DIM, distance to the Individual mean; % in zone refers to the proportion of footfalls that land in the expected loading zone for that surface (see Fig. 2A). The average PR, DIM and % in zone across the cranial and caudal surfaces are shown; †indicates a significant difference between the metacarpus and radius.

Separate measures of variability: TSO, tensile strain orientation; FTSR, fractional tensile strain ratio. Variance values for TSO and FTSR are multiplied by 10^3.

acted close to the bone's long axis (TSO: 72±5° and 68±11°, respectively; Table 2). The overall loading pattern of the radius was also similar to that recorded for the outdoor activities, with the caudal surface loaded predominantly in axial compression (FTSR: 0.31±0.02; TSO: 81±1°) and the cranial surface loaded mostly in tension (FTSR: 0.63±0.02; TSO: 10±3°), with both principal strains acting close to the bone's long axis.

Variability in strain pattern

Outdoor *versus* treadmill

The variability in loading pattern, or the two-dimensional spread of the data, was greater during outdoor behaviors than during treadmill locomotion. This was true for the cranial and caudal surfaces of both bones, using participation ratio (PR; Fig. 5A) or distance to the individual mean (DIM, Fig. 5B) to evaluate the data spread (both yielded similar results). The difference between outdoor and treadmill PR within each surface was significant in three of the four comparisons (caudal metacarpus and cranial/caudal radius; Mann–Whitney *U*-tests, $P<0.05$), and the cranial radius had significantly higher DIM during outdoor than treadmill locomotion ($P<0.05$). All four surfaces had approximately the same PR for both outdoor (mean across the four surfaces: 62.6±9.9; Fig. 5A) and treadmill locomotion (mean: 12.8±3.0; Fig. 5A).

The percentage of footfalls landing in the expected bone loading zone was not significantly different between outdoor and treadmill conditions for any of the four surfaces (Fig. 5C). The variance in tensile strain orientation (TSO, normalized to 90°) was significantly greater during outdoor trials compared to treadmill trials in 11 of the 14 individual comparisons (Fig. 6A). Variance in FTSR was significantly greater during outdoor trials than during treadmill trials in 12 of 14 comparisons (Fig. 6B).

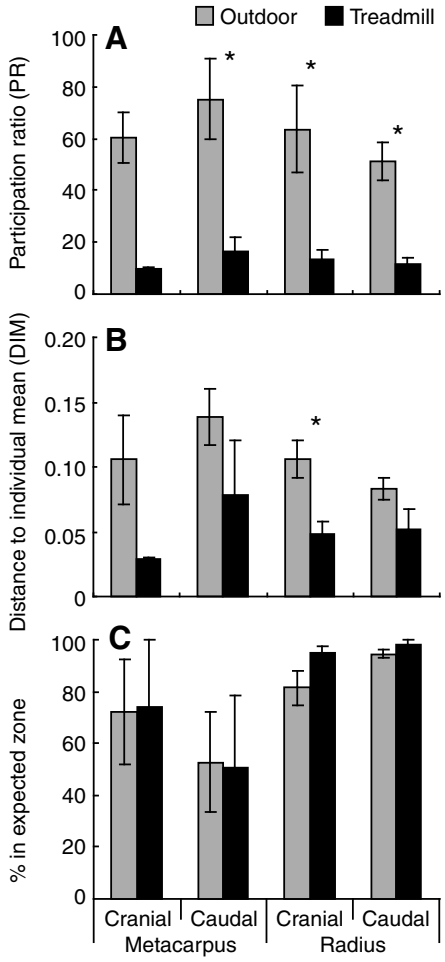

Fig. 5. Composite measures of variability in loading pattern, shown for the cranial and caudal midshaft surfaces of both bones during outdoor (grey) and treadmill (black) locomotion. (A) Participation ratio (PR) and (B) Distance to Individual Mean (DIM) are measures of two-dimensional spread, and (C) percentage of footfalls that land in the expected loading zone indicates how consistently individual footfalls land within the expected range of TSO and FTSR. For both measures of 2D spread (A,B), outdoor footfalls are more variable than those of treadmill locomotion, but not all comparisons are significant because of low degrees of freedom (*significant difference, $P<0.05$). (C) For both bones the percentage of footfalls landing in the expected loading zone is not significantly different between outdoor and treadmill conditions. Values shown are means ± s.e.m.

Radius *versus* metacarpus

Curvatures in the medio-lateral (M-L) and cranio-caudal (C-C) directions were greater for the radius than the metacarpus according to *t*-tests (M-L: radius 0.24±0.05, metacarpus 0.09±0.01, $P=0.039$; C-C: radius 1.27±0.09, metacarpus 0.13±0.01, $P<0.0001$; Fig. 2B). There were no significant differences in PR between the radius and metacarpus for comparisons within a bone surface, nor in average PR for the cranial and caudal surfaces (average outdoor PR: 69±10 metacarpus *versus* 57±8 radius, $P=0.35$; average treadmill PR: 14±3 metacarpus *versus* 12±2 radius, $P=0.72$; Table 2). The average DIM was also not significantly different for within individual bone surface comparisons (average outdoor DIM: 0.12±0.02 metacarpus *versus* 0.09±0.01 radius, $P=0.12$; average treadmill DIM: 0.06±0.03 metacarpus *versus* 0.05±0.01 radius, $P=0.69$; Table 2).

The percentage of footfalls in the expected bone-loading zone, averaged across the cranial and caudal surfaces, was significantly higher in the radius than the metacarpus for both outdoor locomotion (88.6±3.7% radius *versus* 61.2±13.5% metacarpus; $P=0.046$) and treadmill locomotion (96.5±1.6% radius *versus* 60.1±18.2% metacarpus; $P=0.013$; Table 2). During outdoor locomotion (grey bars), although the variance in TSO averaged across the cranial and caudal surfaces was similar between the bones (Fig. 6C), the variance in FTSR averaged across cranial and caudal surfaces was significantly greater in the metacarpus than the radius (Fig. 6D). During treadmill locomotion (black bars) the average variance in TSO was larger in the metacarpus than the radius (Fig. 6C), but the average variance in FTSR across these midshaft surfaces was not significantly different between the two bones (Fig. 6D).

Variability in local bone strain magnitude

Outdoor *versus* treadmill

Out of 22 individual bone surface comparisons of the variance in strain magnitude between outdoor and treadmill locomotion for the seven goats, the variance in strain magnitude for outdoor, non-steady locomotion was greater in all but two cases. However, the difference in variance between outdoor and treadmill was significant in only half of those comparisons according to *F*-tests (4 of 8 metacarpus, 7 of 14 radius).

Radius *versus* metacarpus

Mean peak strain magnitudes during outdoor behaviors were not significantly different from those experienced during treadmill locomotion. This was true on the three midshaft surfaces of both the metacarpus and the radius (Table 3). The similarity between conditions is illustrated by the frequency distributions for the

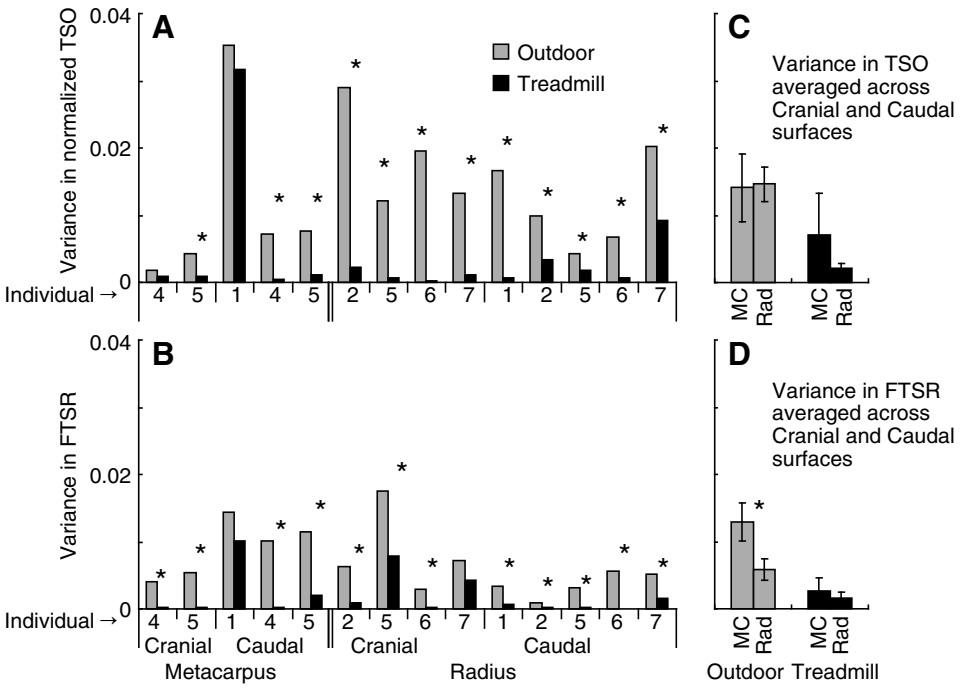

Fig. 6. Within-individual variability in loading pattern in terms of (A) variance in tensile strain orientation (TSO; normalized to 90°) and (B) variance in fractional tensile strain ratio (FTSR). Values are shown when outdoor (grey) and treadmill (black) data for the cranial and caudal surfaces of both bones were available for an individual. In most of the within-individual comparisons (TSO: 3 of 5 metacarpus, 8 of 9 radius; FTSR: 4 of 5 metacarpus, 8 of 9 radius), the variance in these dimensions during outdoor locomotion is significantly greater than during treadmill locomotion (*significant difference in variances, according to *F*-tests). (C) Variance in TSO averaged across individuals for the cranial and caudal surfaces of each bone was not significantly different between the metacarpus (MC) and radius (Rad) for either experimental condition. (D) Variance in FTSR averaged across individuals for the cranial and caudal surfaces was low and not significantly different between bones during treadmill locomotion, but was significantly lower (P=0.037) in the radius during outdoor locomotion.

metacarpus (Fig. 7) and radius (Fig. 8), comparing outdoor and treadmill conditions. During outdoor locomotion, the cranial and caudal surfaces of the metacarpus experienced mean absolute magnitudes that were similar to each other (256±54 με and 281±43 με, respectively; Table 3) and to the cranial surface of the radius (281±95 με). However, the caudal surface of the radius experienced a greater absolute mean peak strain magnitude (581±67 με). The medial surfaces of the metacarpus and radius also experienced absolute peak strain magnitudes in this range (567±77 με and 656±111 με, respectively; Table 3).

Axial and bending strains

During outdoor locomotion, the mean bending strain in the radius was 5.3 times greater than that of the metacarpus (446±82 με and 84±24 με, respectively, P=0.015; Fig. 9A; Table 4), while the axial strains were not different (–167±41 με radius and –210±39 με metacarpus, P>0.05; Fig. 9A; Table 4). The metacarpus showed more variability in bending strain than did the radius (CV=1.06 in the metacarpus *versus* 0.33 in the radius), but the two bones had a similar CV for axial strains (–0.66 metacarpus, –0.59 radius; Fig. 9B; Table 4). Bending strains in the straighter metacarpus were lower than the axial strains (bending to axial strain ratio=0.40), but this difference was not significant (P=0.051). By contrast, the bending strains in the radius were significantly greater than the axial strains (bending to axial strain ratio=2.67; P=0.023).

During treadmill locomotion, the mean bending strain in the radius was 11.4 times greater than in the metacarpus (493±68 με and 43±31 με, respectively, P=0.012; Fig. 9C; Table 4), whereas axial

Table 3. Frequency distribution for the peak strain magnitudes for outdoor *versus* treadmill conditions

		Outdoor						Treadmill					
		N	Mean ± s.e.m.	Median	Min	Max	IQR	*N*	Mean ± s.e.m.	Median	Min	Max	IQR
Metacarpus	Cranial	3	256±54	245	22	1173	149	2	230±46	198	99	538	157
	Caudal	4	281±43	219	31	1385	146	3	202±49	177	73	381	149
	Medial	3	567±77	506	84	1908	495	4	585±106	487	121	1342	465
Radius	Cranial	4	281±95	202	32	1043	181	5	370±123	280	46	999	395
	Caudal	5	581±67	533	80	1746	331	5	625±61	593	206	1298	217
	Medial	5	656±111	580	51	1945	418	5	709±113	644	210	1671	339

Values are for peak absolute principal strain magnitudes (με) on the cranial and caudal surfaces and peak absolute axial strain magnitudes for the medial surfaces. The means for the outdoor *vs* treadmill for each surface were not significant (P>0.05 in all cases). The median, minimum, maximum and inter-quartile range (IQR) are shown for pooled data (sample sizes from Table 1) from each surface. IQR indicates the difference between the 75th and 25th percentile for each relative frequency distribution.

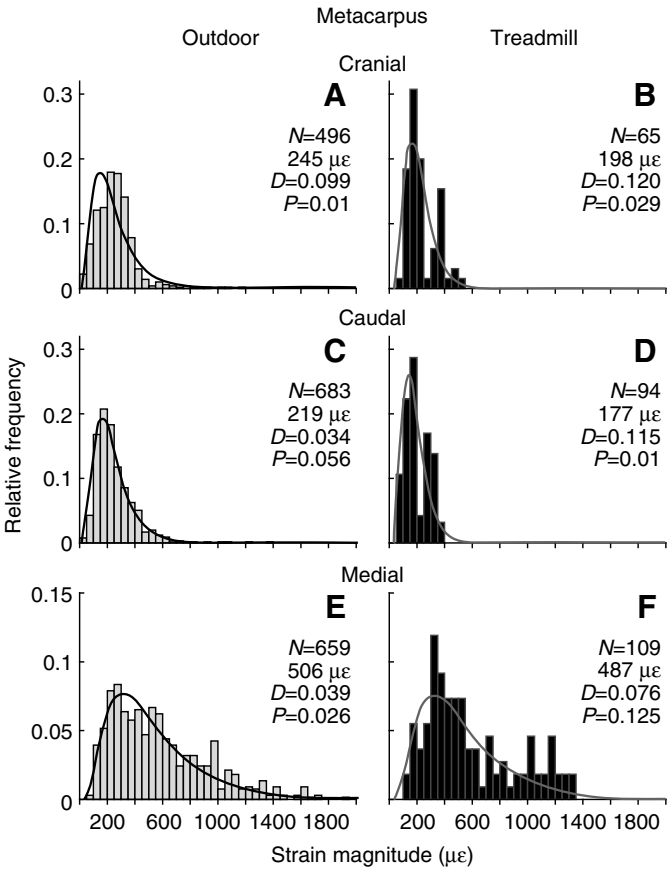

Fig. 7. Frequency distributions of strain magnitudes for the cranial, caudal and medial surfaces of the metacarpus, for both outdoor and treadmill locomotion. Peak principal strain magnitudes (absolute magnitudes of compressive or tensile principal strains) are shown for cranial and caudal surfaces (A–D) and peak axial strain magnitudes are shown for medial surfaces (E,F). These distributions contain pooled data across all behaviors and individuals, providing an estimate of the distribution pattern for the population of strains recorded at each bone surface. During both outdoor and treadmill locomotion, strains in all three surfaces appeared to be log-normally distributed, although only in the cases where $P>0.05$ (caudal outdoor, C, and medial treadmill, F) was the fit not significantly different from a standard lognormal distribution. The pooled sample size and the median are shown, as well as the *D*-statistic from the KSL goodness-of-fit test, which indicates that the outdoor data had smaller deviations from the best-fit lognormal curves than the treadmill data.

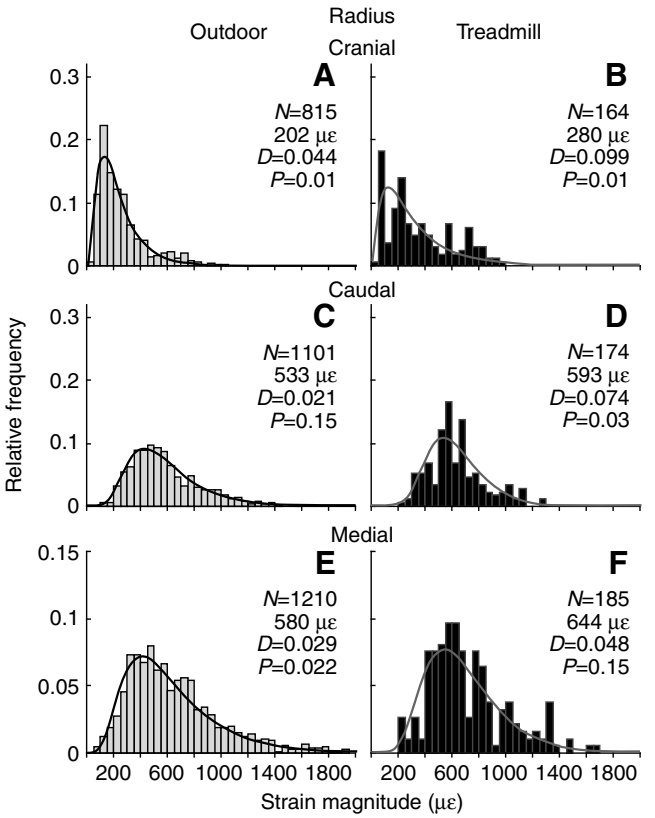

Fig. 8. Frequency distributions of strain magnitudes for the cranial, caudal and medial surfaces of the radius. Details of these distributions and the values shown are the same as in Fig. 7. Though all six distributions are skewed to the right and appear to fit a lognormal distribution, only the caudal surface during outdoor locomotion (C; $P=0.15$) and the medial surface during treadmill locomotion (F, $P=0.15$) are not significantly different than a standard lognormal distribution. As in the metacarpus, all of the outdoor distributions had smaller deviations (according to the D statistic) from the log-normal curves than the corresponding treadmill distributions, probably because the larger sample size for the outdoor data.

strains were again not different (–123±70 με radius and –194±8 με metacarpus, $P>0.05$; Fig. 9C; Table 4). The metacarpus also showed more variability in bending strain than the radius during treadmill locomotion (CV=0.65 in the metacarpus *versus* 0.23 in the radius), but the CVs for axial strains were similar (–0.35 metacarpus, –0.24 radius; Fig. 9D; Table 4). Bending strains in the metacarpus were lower than the axial strains (bending to axial strain ratio=0.22), but we could not test the significance of this difference because of a low sample size. The bending strain of the radius was significantly larger than its axial strain (bending to axial strain ratio=4.02; $P=0.003$).

Strain magnitude distributions

The distribution of strain magnitudes for the natural, outdoor behaviors was right skewed and appeared to fit a lognormal distribution for the cranial and caudal surfaces of both the metacarpus (Fig. 7A,C) and radius (Fig. 8A,C). This fit was significant on the caudal surfaces ($P=0.056$ metacarpus, $P=0.15$ radius; Table 3) but not on the cranial surfaces ($P=0.01$ for both metacarpus and radius). The strain magnitudes also appeared to be lognormally distributed on the medial surfaces for both bones (Fig. 7E,F and Fig. 8E,F), but the fits were not significant. During treadmill locomotion the strain magnitude distributions on the cranial and caudal surfaces of both bones did not fit a lognormal distribution. However, the medial surfaces of both bones showed significant lognormal distributions ($P=0.125$ metacarpus, $P=0.15$ radius; Table 3). The D-statistic of the KSL goodness of fit test gives a measure of the greatest deviation from the standard lognormal distribution. On each surface of both bones this value was lower for outdoor *versus* treadmill conditions (Figs 7, 8). Consequently, outdoor strain magnitude distributions deviated less from lognormal than the treadmill distributions.

DISCUSSION

In this study we measured strain patterns and magnitudes in two goat forelimb bones during a variety of natural, outdoor behaviors to explore how bone curvature influences the predictability of loading pattern and magnitude during non-steady locomotion. We hypothesized that peak principal strains in the goat radius and

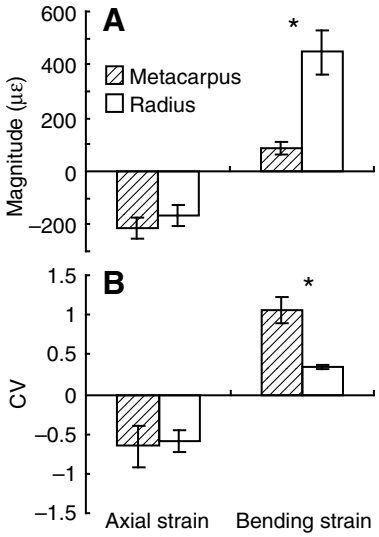

Fig. 9. (A) Axial *versus* bending strain components for the metacarpus and the radius during outdoor activities. Although axial strain components did not differ between bones, bending strain in the radius (white bars) was significantly greater than in the metacarpus (hatched bars). (B) The coefficient of variation (CV) of the axial and bending strain components for both bones during outdoor activities. Variability in axial strains was similar between bones, but the variability in bending strain was significantly greater in the straighter metacarpus *versus* the curved radius.

metacarpus would be more variable in pattern and magnitude during outdoor behaviors compared to treadmill behaviors. We also predicted that during outdoor locomotion the curved radius would be less variable in strain pattern but would experience higher peak strains compared to the straighter metacarpus. We found that outdoor behaviors resulted in more variability in loading pattern but not more variability in strain magnitude compared to treadmill locomotion. We also found that strains in the radius occurred more frequently in the expected loading zone compared to the metacarpus, and the radius showed significantly less variability in bending strains during outdoor locomotion. However, the orientations of peak principal strains derived from a broad range of natural activities were not less variable overall in the radius than in the metacarpus. Although the curved radius did experience maximum peak principal strains of a greater magnitude than the metacarpus, these high magnitude loading events (above the median strain level) were more likely to occur within a predictable range of loading orientations in the curved radius than in the straighter metacarpus.

Bone strain variability during steady *versus* non-steady locomotion

We hypothesized that strain patterns measured during outdoor locomotion would be more variable because non-steady behaviors may cause the forelimbs to contact the ground in unusual positions or angles, resulting in variable ground reaction force orientations relative to the limb and, as a consequence, more varied strain orientations (TSO) and dominant strain types (FTSR; Fig. 4). The softer, uneven substrate of the outdoor arena compared to the treadmill may be another factor causing unpredictable limb loading events. Our composite measures of the variability of midshaft bone loading pattern, participation ratio (PR) and distance to the individual mean (DIM), support this hypothesis (Fig. 5A,B), as does the variability in the two separate dimensions of loading pattern: tensile strain orientation (TSO) and fractional tensile strain ratio (FTSR). Given the differences in variance of these parameters between outdoor and treadmill locomotion, it is interesting that the proportion of footfalls in the expected bone loading zone is nearly the same for both conditions (Fig. 5C) suggesting that the general loading pattern for the cranial and caudal surfaces of both forelimb bones is predictable, even during non-steady behaviors. This is consistent with previous studies in which surface midshaft strains recorded in the long bones of a number of species over a range of speeds and gaits showed uniform strain patterns (Lanyon and Baggott, 1976; Rubin and Lanyon, 1982; Biewener and Taylor, 1986). Additionally, the mean values for FTSR and TSO were nearly identical for the treadmill and outdoor activities. Although treadmill locomotion does not entirely capture the variability in loading orientations and dominant strain types that result from outdoor, non-steady locomotor behaviors, the results for these goat forelimb bones indicate that treadmill locomotion can serve as a reasonable approximation for some natural locomotor activities.

We expected both bones would experience higher peak principal strains during outdoor behaviors because these can include more high-intensity activities such as jumping down or sudden decelerations, based on previous work showing that strains increase when non-steady behaviors such as jumping (Biewener et al., 1983a; Biewener et al., 1988) and accelerations (Biewener et al., 1983b) are examined. Consistent with this, the tails of the outdoor frequency distributions of peak principal strains (cranial and caudal surfaces) and peak compressive strains (medial surface) extended further to the right than the corresponding treadmill distributions (Figs 7, 8). Hence, a relatively few high magnitude loading events recorded during outdoor activity produced greater peak strains than the most vigorous gallops recorded on the treadmill. However, these less frequent high magnitude events were insufficient to significantly affect the overall mean peak strain magnitudes of the distributions,

Table 4. Axial *versus* bending strain magnitudes across bones and experimental condition

	Metacarpus		Radius	
	Outdoor	Treadmill	Outdoor	Treadmill
N	3	2	4	5
Bending strain	84±24	43±31	446±82†	493±68†
Axial strain	–210±39	–194±8	–167±41	–123±70
Bending to axial ratio (magnitudes)	0.40	0.22	2.67	4.02
CV axial	–0.66±0.26	–0.35±0.01	–0.59±0.14	–0.24±0.16
CV bending	1.06±0.16	0.65±0.05	0.33±0.01††	0.23±0.02**,†††

All values are means ± s.e.m. CV, coefficient of variation.
Asterisks indicate significant differences between outdoor *vs* treadmill values for the same bone (*P<0.05, **P<0.01, ***P<0.001).
Daggers indicate significant differences between the metacarpus and radius within the same experimental condition ($^{\dagger}P$<0.05, $^{\dagger\dagger}P$<0.01, $^{\dagger\dagger\dagger}P$<0.001).

as these were similar on all three surfaces of both bones for outdoor and treadmill locomotion (Table 3).

We also hypothesized that many of these high-intensity events would occur during the outdoor activities, causing greater variability in the frequency distribution of peak strain magnitudes compared to treadmill locomotion. This hypothesis was partially supported, as half of the within-individual comparisons showed a significant difference in variance between outdoor and treadmill locomotion (figure not shown). The variability (CV) of bending strain in the radius was also significantly greater during outdoor *versus* treadmill locomotion. The same is probably true for the metacarpus; however, a less robust sample size prevented a statistical comparison for this bone (Table 4). These findings suggest that the variable nature of outdoor behaviors may increase the risk of failure compared to steady state, not because the mean principal strains are higher than in treadmill behaviors but because of occasional extreme principal strains and because these outdoor behaviors can engender more variable bending strains than treadmill behaviors. The extent to which more variable bending increases the overall peak strain magnitude within a bone, therefore, may increase a bone's risk of failure.

Effect of bone curvature on the variability of strain pattern and magnitude

Strain pattern variability

During both outdoor and treadmill locomotion, the two goat forelimb bones are dominated by axial loads that induce intrinsic bending in proportion to their longitudinal curvature. Whereas the straight metacarpus experiences compression on the cranial, caudal and medial surfaces, reflecting overall axial compression, the radius experiences compression on its concave caudal surface, as well as its medial cortex, and tension on its convex cranial surface, reflecting bending that results primarily from axial loading about the bone's longitudinal curvature, rather than extrinsic bending loads (Fig. 2A, Figs 3, 4). These strain distributions are consistent with previous findings in which the predominant loading mode in the ungulate radius was axial compression with superimposed cranio-caudal bending (Lanyon and Baggott, 1976; Goodship et al., 1979; Lanyon et al., 1982; Rubin and Lanyon, 1982; Biewener et al., 1983a; Biewener and Taylor, 1986; Bertram and Biewener, 1988; Bertram and Biewener, 1992).

We hypothesized that during outdoor locomotion, the radius would be more predictable in terms of overall midshaft strain pattern than the metacarpus because the curvature of the radius, and probably the surrounding musculature, would restrict the strain orientations and nature of the strains (tensile *versus* compressive) to predictable ranges, whereas the patterns in the straighter metacarpus would be more variable. This was based on previous work showing that variation in loading orientation during jumping is greater in straighter bones, such as the metacarpus (Biewener et al., 1983a) and metatarsus (Biewener et al., 1988). The greater variability in these bones likely results from having little longitudinal curvature, which diminishes their ability to restrict bending to a fixed direction (Bertram and Biewener, 1988). Consistent with this, our data show that the percentage of footfalls in the expected bone loading zone is significantly higher for the radius than the metacarpus for both outdoor and treadmill locomotion (Fig. 4 and Table 2). This suggests that the curved radius restricts the *overall* loading distribution of midshaft strains more than the straighter metacarpus, such that a larger proportion of footfalls are constrained to within a more predictable range of strain patterns.

However, variability in loading pattern, as assessed by the average PR and DIM for the cranial and caudal surfaces, was not different between the metacarpus and radius for within location comparisons (Fig. 5A,B; Table 2). Examining the separate dimensions that make up these measures of pattern variability reveals why they do not differ. Although the variance in FTSR (Fig. 6D) for the metacarpus is significantly greater than that of the radius, the variance in TSO is almost identical for the two bones (Fig. 6C). Since PR and DIM comprise both of these dimensions, it is not surprising that similarity in one of these dimensions results in no significant difference in the composite measures of loading pattern variability. Additionally, these findings indicate that during outdoor, natural behaviors, the curved radius is able to constrain the strain ratios (FTSR) more than the straighter metacarpus, but does not constrain the variability in orientation of the principal strain (TSO) more than in the metacarpus. This suggests that under variable locomotor conditions a curved bone will not see remarkably less varied principal strain orientations than a straight bone, but the curved bone will restrict the ratio of tension to compression to within a more predictable range for any given footfall, whereas a straight bone will experience more variable tension-to-compression ratios. In this case, a critical factor for preventing failure during non-steady activities may be the specific bone microstructure and collagen fiber orientation in the cortices of straight bones compared with curved bones (Skedros et al., 2006), which is a level of detail not examined in our study.

This difference in the effect of longitudinal bone curvature on TSO *versus* FTSR helps explain why a small percentage of outdoor footfalls are scattered outside the expected loading zones (Fig. 4, grey diamonds). Recorded strains have similar ranges of TSO values for the two forelimb bones, but more constrained FTSR values for the radius (Fig. 4C,D) than the metacarpus (Fig. 4A,B). As an *ad hoc* experimental analysis, we hypothesized that the outlying footfalls might be of lower magnitude, such that the eccentric loading orientations were not as consequential to the integrity of the bone (lower risk of failure). This analysis is discussed further below.

In addition to longitudinal curvature, two other anatomical features that are likely to affect loading predictability are the organization of surrounding musculature and the cross-sectional geometry of each bone (Bertram and Biewener, 1988). The radius has an array of digital flexors and extensors originating from its proximal end, whereas the metacarpus has only the interosseous muscle on its palmar surface, with flexor and extensor tendons passing over both ends of the bone. Based on the fixed attachment points of the muscles associated with the radius, it is possible that its loading environment is dominated by muscular forces more than in the metacarpus, contributing to the greater loading predictability of the radius. Additionally, the two bones have different cross-sectional geometries, with the metacarpus more circular and the radius more elliptical. The more elliptical cross-sectional shape of the radius, therefore, also likely contributes to a more restricted cranio-caudal bending. However, neither of these factors were quantified and explored in this study. Nevertheless, analysis of cross-sectional strain distributions and bending orientation with respect to bone shape and muscle–tendon organization is deserving of future study.

Peak strain magnitudes and variability

We hypothesized that during outdoor locomotion the radius would experience greater peak strains compared to the metacarpus based on the prediction that the radius would experience greater bending compared to the metacarpus (Biewener et al., 1983a; Lanyon, 1987). We evaluated this for the caudal midshaft cortex of each bone because compression due to bending of this cortex in the radius is augmented by axial compression, resulting in greater net strain. By

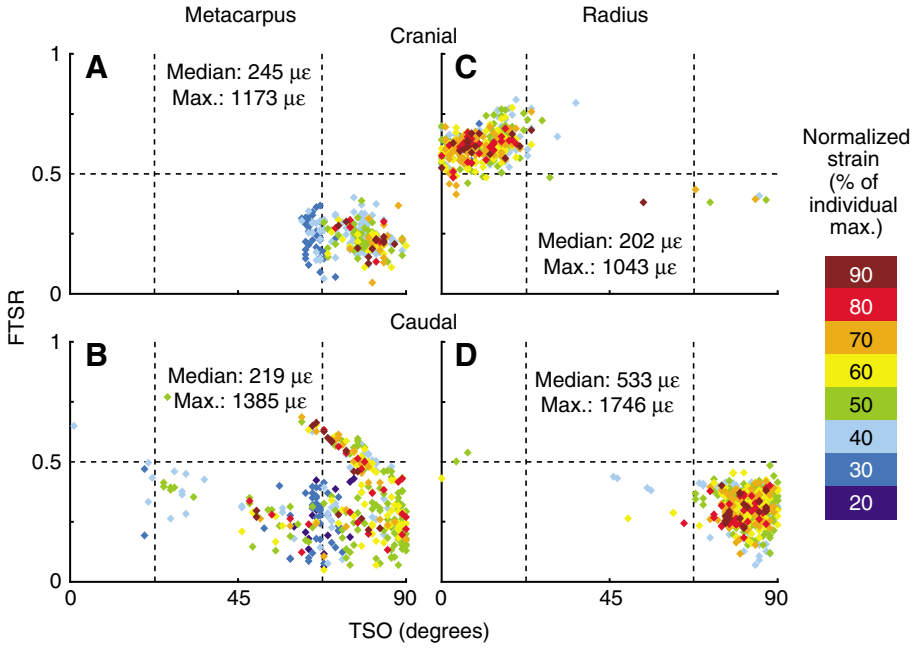

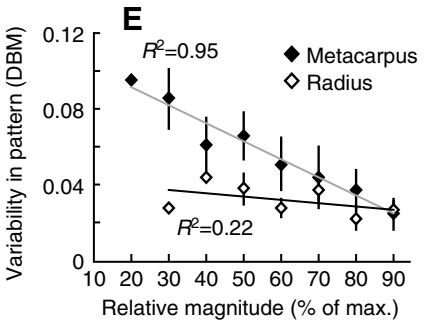

Fig. 10. (A–D) FTSR *versus* TSO for outdoor loading events having magnitudes greater than the pooled median, plotted within bins representing normalized strain magnitudes, where cool colors are lower magnitudes and warm colors are higher magnitudes, quantified as a percentage of the maximum value recorded for each bone site. The minimum (median) and maximum strain values are shown for each bone surface. (E) Variability in strain pattern expressed as distance to the bin mean (DBM) regressed against bin magnitude, represented as a percentage of the maximum strain recorded. DBM values were averaged across the cranial and caudal midshaft surfaces for the metacarpus and the radius.

contrast, bending-induced tension of the cranial cortex is offset by axial compression, resulting in smaller net tensile strains. Consistent with our hypothesis and previous work (Biewener et al., 1983b; Lanyon, 1987; Bertram and Biewener, 1988; Biewener et al., 1988), the cranial surface of the radius experienced similar tensile principal strain magnitudes as the compressive principal strains recorded in the cranial and caudal metacarpus (Fig. 9A), whereas the caudal radius experienced higher peak compressive strains than the metacarpus. As expected, we also found significantly greater bending strains in the radius than the metacarpus (Fig. 9A). Although greater strains due to bending were measured in the radius, the coefficient of variation (CV) of this strain component was lower for the radius than the metacarpus (Fig. 9B). This result strongly supports the hypothesis that longitudinal bone curvature induces a trade-off between load predictability and strain magnitude (Bertram and Biewener, 1988; Bertram and Biewener, 1992). There was no difference in axial strain magnitudes between the two bones, and the CV for axial strain components is the same for both bones, suggesting that differences in bone curvature and the bending strains that are engendered are more important for understanding functional design of these two forelimb bones.

Safety factor, bone curvature and predictability

Failure of a critical structural element, such as a forelimb bone, will presumably carry a substantial biological cost to a terrestrial animal. A critical structural design requirement is that these elements possess suitable safety factors, defined as the ratio of failure strength to their expected maximum load, to reduce the probability of failure. Since one of the primary functions of the limb skeleton is to transmit locomotor forces without yielding or breaking, it might seem advantageous for these bones to be as massive as possible. However, because bone is also metabolically costly to produce, maintain and transport, there is a tradeoff between massive bones conferring a large safety factor and less massive bones that are more economical, but may have a higher probability of failure (Alexander, 1981; Biewener, 1993). The balance between these conflicting demands results in the final architecture of the bone, which strongly influences the nature of the stresses (and strains) that the bone experiences.

It has been suggested that different limb bones may be expected to have different safety factors, probably related to differences in their architecture (Alexander, 1981; Biewener et al., 1983a; Currey, 2002). As discussed above, a limb bone with substantial longitudinal curvature may have greater predictability of loading direction (Bertram and Biewener, 1988; Bertram and Biewener, 1992), which allows the bone to adjust its form and mass *via* remodeling to better maintain functional integrity during natural activities (Lanyon, 1987; Biewener and Bertram, 1993). This process can reduce the probability that a loading event from an especially vigorous behavior will cause a stress that approaches the bone's breaking strength, due to the reduced likelihood of overlap between the positive tail of the frequency distribution of functional bone stresses and the distribution of breaking (or failure) strengths (Alexander, 1981). By reducing loading variability, the mean breaking strength can safely be decreased, allowing more economical costs of maintenance and transport, despite the trade-off of greater stress (or strain).

Our results do not completely support this hypothesis for natural, outdoor locomotor behaviors. We found that while the curved radius has higher bending strains than the straighter metacarpus, it does not have greater predictability of loading orientation (TSO; Fig. 6C). However, in the radius the variability of the dominant strain type (FTSR; Fig. 6D) and the variability in bending strain (CV; Table 4) are indeed less than those of the metacarpus. It is possible that eccentric loading events during outdoor locomotion can produce loading orientations in the medio-lateral direction that are not highly constrained by the cranio-caudal curvature of the radius.

Relationship between strain magnitude and variability in strain pattern

To help explain why a percentage of footfalls are scattered outside the expected bone loading zones, and to address the finding that the curved radius does not constrain loading orientation (TSO) more than the metacarpus, we investigated the relationship between strain magnitude and variability in loading pattern in both bones. Our hypothesis was that higher magnitude loading events would be more constrained in loading pattern, which would reduce the likelihood that high magnitude loads occur substantially off-axis (or with unexpected ratios of tension to compression) and thereby increase the potential risk for damage and/or failure. Accordingly, the strain pattern associated with very low magnitude loading cycles would not be as constrained because they would pose less of a failure risk to the bone.

To explore this hypothesis, we removed loading events with magnitudes below the pooled median magnitude from all of the outdoor footfalls. Plotting TSO against FTSR for the remaining data shows that most of the footfalls with eccentric, off-axis loads that would have landed far from the expected loading zone have been eliminated (compare Fig. 4 with Fig. 10). This indicates that footfalls with highly unexpected TSO or FTSR values were of relatively low magnitude (below the median value for each goat), whereas all of the higher magnitude footfalls (near the median and higher) generally clustered within the expected loading zones (Fig. 10A–D). This finding supports our hypothesis that very low magnitude loading cycles are not as constrained in pattern as higher magnitude loading cycles.

To test this hypothesis further, we grouped the remaining high magnitude events within bins of strain normalized to the individual maximum magnitude (Fig. 10A–D). We then calculated the distance to the bin mean (DBM) for each data point and computed the average DBM as a measure of variability for each midshaft surface of both bones. We regressed DBM against relative strain magnitude (Fig. 10E) and found a strong negative correlation between variability in pattern and magnitude for the metacarpus (R^2=0.95, slope=–0.009, P<0.001), but no correlation for the radius (R^2=0.22, slope=–0.002, P=0.28). This result suggests a difference between the two bones in terms of the degree to which they constrain the loading pattern of footfalls with different magnitudes. Although the radius shows low variability in loading pattern magnitudes near the median and at the highest magnitudes, the metacarpus shows higher variability in loading pattern at magnitudes near the median and less variability at the highest magnitudes. In fact, at the highest magnitudes the variability in loading pattern of the metacarpus is nearly the same as in the radius. Our interpretation is that the curvature of the radius, or other features of its architecture, does not constrain the eccentric, very low magnitude footfalls (below the median; outliers from Fig. 4 not included in Fig. 10) any better than the metacarpus (hence the same PR and DIM) because these footfalls have low risk of causing failure, but it does constrain the TSO and FTSR of loading cycles with magnitudes near the relative median more than the metacarpus. Once the magnitudes are near the maximum, then both bones show constrained loading patterns on those footfalls.

This explains the seemingly conflicting findings that predictability in general loading pattern expressed as a percentage in the expected loading zone (Fig. 5C) differs between the bones (the radius has a higher percentage of footfalls in the expected loading zones than the metacarpus) but PR and DIM do not (Fig. 5A,B). The lowest magnitude footfalls were more likely to occur with extreme loading patterns, and hence, they increased PR and DIM for both bones similarly. The medium magnitude footfalls were more constrained in the radius than in the metacarpus, so this probably was the main factor causing the difference in the percentage in the expected loading zone. The highest magnitude footfalls were highly constrained in loading pattern for both bones, so these did not affect the differences in percentage or in PR and DIM.

It makes intuitive sense that moderate to high magnitude loading cycles (compared to those with very low magnitude) would reveal the difference between the two bones in terms of the functional consequences of curvature. High magnitude loading events with greater strain rates have greater influence on bone modeling and remodeling than sedentary activity (Rubin and Lanyon, 1982; Turner et al., 1995; Mosley and Lanyon, 1998). However, in this study it was the medium magnitude loading events, which occurred with the greatest frequency (Figs 7, 8), that best demonstrate the difference between the bone morphologies. The very low magnitude loading events had unpredictable loading patterns in both bones (these would likely correspond to the sedentary activity in the papers cited above), but the medium magnitude loading events were constrained in loading pattern to a greater extent in the radius than the metacarpus. The highest magnitude loading events were constrained about the same for each bone. Evidently, the difference in bone morphology is the most important at magnitudes near the median, which corresponds to those loading events that occur with the greatest relative frequency (Figs 7, 8). This constraint on loading pattern may arise purely through bone morphology, or it may arise partially through behavioral adjustment in limb position: when the animal expects a moderate to high magnitude limb load, it may position its limb to align more closely with the ground reaction force in order to reduce the chance of a high magnitude event causing damage at a detrimentally aberrant strain orientation. The radius and metacarpus exhibit similar predictability for very low magnitude events (below the median), with both experiencing many eccentric loading orientations, perhaps because these events pose little threat to the structural integrity of the bone.

Functional strain magnitudes are lognormally distributed

Strain magnitude frequency distributions for all midshaft surfaces of the radius and metacarpus derived from outdoor behaviors fit a standard lognormal distribution curve. To a certain extent, strain magnitudes derived from treadmill behaviors were also lognormally distributed. However, the outdoor data fit their respective curves more closely than the corresponding treadmill data, which is probably a consequence of the larger sample sizes that were obtained for the outdoor strain data. It is likely that treadmill distributions would approach a lognormal curve with larger samples. Even so, because of the comparatively large sample sizes, strain magnitudes for only a few bone surfaces showed significant goodness of fit tests (increased sample size increases the test's sensitivity to small deviations from the standard curve and can, therefore, cause 'non-significant' test results). Visual inspection of the strain magnitude frequency distributions (Figs 7, 8) reveals a strong fit to the lognormal distribution curves determined for each bone surface.

Our finding that the frequency distributions of functional bone strain magnitudes during natural behaviors fit a lognormal distribution supports Alexander's (Alexander, 1981) model predicting that natural selection minimizes the associated costs of a given skeletal structure (the cost of growing and using the structure, in addition to the cost of failure). It is possible that these positively skewed distributions of peak strain frequencies reduce the amount of overlap between expected loads and the probability distribution of skeletal breaking strains (Biewener, 1993), such that a bone is

less likely to experience a load that is close to its yield or failure strength, increasing its safety factor (Alexander, 1981).

The daily locomotor activities of many terrestrial animals in the wild are sporadic and may not reflect the behaviors elicited in controlled laboratory treadmill experiments. Wild goats, along with many other terrestrial herbivores, spend most of their time in low-energy behaviors such as walking, feeding, resting, and ruminating (Shi et al., 2003). Some goat species live in natural habitats consisting of mountainous regions with rocky cliffs, steep inclines and variable terrain (Alexander, 1995), where non-steady locomotor behaviors, such as jumping and climbing, are probably quite important. Therefore, although low-magnitude bone strains are experienced much of the time, it is important to evaluate the performance of skeletal elements under a range of natural conditions that include high magnitude loading events in order to better understand the consequences and possible selection pressures on bone architecture and design.

Our study and results provide a starting point for future analysis of bone loading patterns across a variety of non-steady and steady locomotor behaviors. They provide the first direct measurements of loading magnitude frequency distributions of structural elements for natural behaviors to test concepts and a model for biological safety factors first proposed by Alexander (Alexander, 1981). Our findings provide initial support for this model. They also explore the basis of bone strain variability with respect to variation in locomotor behavior and long bone curvature (Bertram and Biewener, 1988). However, as other features, such as bone cross-sectional shape and musculotendinous organization, are also likely important to the pattern and variation of strain experienced by a bone, these should also be evaluated in future work.

LIST OF ABBREVIATIONS

CC	cranio-caudal
CV	coefficient of variation
DBM	distance to the (magnitude) bin mean
DIM	distance to the individual mean
FTSR	fractional tensile strain ratio
GRF	ground reaction force
ML	medio-lateral
PR	participation ratio
TSO	tensile strain orientation
$\mu\epsilon$	microstrain, strain $\times 10^{-6}$
υ	angle between principal strain angle and the long axis of the bone

We would like to thank Stephanie Schur, Tatiana Bartch and Keith Egan for assisting with data collection and analysis, everyone at the Concord Field Station for discussion and help with surgeries, and Pedro Ramirez for his excellent care of the animals. We would also like to thank Tim Higham and Andrew Carroll for providing useful feedback on the manuscript, as well as Luke Mahler for helpful discussion about measures of variability.

REFERENCES

Alexander, R. McN. (1981). Factors of safety in the structure of animals. *Sci. Prog. Oxford* **67**, 109-130.
Alexander, R. McN. (1995). Leg design and jumping technique for humans, other vertebrates and insects. *Philos. Trans. R. Soc. Lond. B Biol. Sci.* **347**, 235-248.
Bertram, J. E. A. and Biewener, A. A. (1988). Bone curvature: sacrificing strength for load predictability? *J. Theor. Biol.* **131**, 75-92.
Bertram, J. E. A. and Biewener, A. A. (1992). Allometry and curvature in the long bones of quadrupedal mammals. *J. Zool. Lond.* **226**, 455-467.
Biewener, A. A. (1992). *In vivo* measurement of bone strain and tendon force. In *Biomechanics: Structures and Systems: A Practical Approach* (ed. A. A. Biewener), pp. 123-147. Oxford: Oxford University Press.
Biewener, A. A. (1993). Safety factors in bone strength. *Calcif. Tissue Int.* **53**, S68-S74.
Biewener, A. A. and Bertram, J. E. (1993). Skeletal strain patterns in relation to exercise training during growth. *J. Exp. Biol.* **185**, 51-69.
Biewener, A. A. and Dial, K. P. (1995). *In vivo* strain in the humerus of pigeons *Columba livia* during flight. *J. Morphol.* **225**, 61-75.
Biewener, A. A. and Taylor, C. R. (1986). Bone strain: a determinant of gait and speed? *J. Exp. Biol.* **123**, 383-400.
Biewener, A. A., Thomason, J. J. and Lanyon, L. E. (1983a). Mechanics of locomotion and jumping in the forelimb of the horse (*Equus*): *in vivo* stress developed in the radius and metacarpus. *J. Zool. Lond.* **201**, 67-82.
Biewener, A. A., Thomason, J. J., Goodship, A. and Lanyon, L. E. (1983b). Bone stress in the horse forelimb during locomotion at different gaits: a comparison of two experimental methods. *J. Biomech.* **16**, 565-576.
Biewener, A. A., Thomason, J. J. and Lanyon, L. E. (1988). Mechanics of locomotion and jumping in the horse (*Equus*): *in vivo* stress in the tibia and metatarsus. *J. Zool. Lond.* **214**, 547-565.
Blob, R. W. and Biewener, A. A. (1999). *In vivo* locomotor strain in the hindlimb bones of *Alligator mississippiensis* and *Iguana iguana*: implications for the evolution of limb bone safety factor and non-sprawling limb posture. *J. Exp. Biol.* **202**, 1023-1046.
Burr, D. B., Robling, A. G. and Turner, C. H. (2002). Effects of biomechanical stress on bones in animals. *Bone* **30**, 781-786.
Carter, D. R. (1987). Mechanical loading history and skeletal biology. *J. Biomech.* **20**, 1095-1107.
Carter, D. R., Smith, D. J., Spengler, D. M., Daly, C. H. and Frankel, V. H. (1980). Measurement and analysis of *in vivo* bone strains on the canine radius and ulna. *J. Biomech.* **13**, 27-31.
Ciampaglio, C. N., Kemp, M. and McShea, D. W. (2001). Detecting changes in morphospace occupation patterns in the fossil record: characterization and analysis of measures of disparity. *Paleobiology* **27**, 695-715.
Currey, J. D. (2002). *Bones: Structure and Mechanics*. Princeton, NJ: Princeton University Press.
Goodship, A. E., Lanyon, L. E. and MacFie, H. (1979). Functional adaptation of bone to increased stress. An experimental study. *J. Bone Joint Surg. A* **61**, 539-546.
Gross, T. S., McLeod, K. J. and Rubin, C. T. (1992). Characterizing bone strain distributions *in vivo* using three triple rosette strain gages. *J. Biomech.* **25**, 1081-1087.
Lanyon, L. E. (1976). The measurement of bone strain *in vivo*. *Acta Orthop. Belgica* **42**, 98-108.
Lanyon, L. E. (1987). Functional strain in bone tissue as an objective, and controlling stimulus for adaptive bone remodeling. *J. Biomech.* **20**, 1083-1093.
Lanyon, L. E. and Baggott, D. G. (1976). Mechanical function as an influence on the structure and form of bone. *J. Bone Joint Surg. B* **58**, 436-443.
Lanyon, L. E., Goodship, A. E., Pye, C. J. and MacFie, J. H. (1982). Mechanically adaptive bone remodelling. *J. Biomech.* **15**, 141-154.
Lieberman, D. E., Pearson, O. M., Polk, J. D., Demes, B. and Crompton, A. W. (2003). Optimization of bone growth and remodeling in response to loading in tapered mammalian limbs. *J. Exp. Biol.* **206**, 3125-3138.
Main, R. P. and Biewener, A. A. (2004). Ontogenetic patterns of limb loading, *in vivo* bone strains and growth in the goat radius. *J. Exp. Biol.* **207**, 2577-2588.
Mosley, J. R. and Lanyon, L. E. (1998). Strain rate as a controlling influence on adaptive modeling in response to dynamic loading of the ulna in growing male rats. *Bone* **23**, 313-318.
Mosley, J. R., March, B. M., Lynch, J. and Lanyon, L. E. (1997). Strain magnitude related changes in whole bone architecture in growing rats. *Bone* **20**, 191-198.
Rice, W. R. (1989). Analyzing tables of statistical tests. *Evolution* **43**, 223-225.
Robling, A. G., Duijvelaar, K. M., Geevers, J. V., Ohashi, N. and Turner, C. H. (2001). Modulation of appositional and longitudinal bone growth in the rat ulna by applied static and dynamic force. *Bone* **29**, 105-113.
Rohlf, F. J. and Sokal, R. R. (1981). *Statistical Tables*. New York: Freeman.
Rubin, C. T. and Lanyon, L. E. (1982). Limb mechanics as a function of speed and gait: a study of functional strains in the radius and tibia of horse and dog. *J. Exp. Biol.* **101**, 187-211.
Shi, J., Dunbar, R. I. M., Buckland, D. and Miller, D. (2003). Daytime activity budgets of feral goats (*Capra hircus*) on the Isle of Rum: influence of season, age, and sex. *Can. J. Zool.* **81**, 803-815.
Skedros, J. G., Dayton, M. R., Sybrowsky, C. L., Bloebaum, R. D. and Bachus, K. N. (2006). The influence of collagen fiber orientation and other histocompositional characteristics on the mechanical properties of equine cortical bone. *J. Exp. Biol.* **209**, 3025-3042.
Sokal, R. R. and Rohlf, F. J. (1981). *Biometry*. New York: Freeman.
Turner, C. H., Owan, I. and Takano, Y. (1995). Mechanotransduction in bone-role of strain rate. *Am. J. Physiol. Endocrinol. Metab.* **269**, E438-E442.